https://doi.org/10.5607/en22035
Exp Neurobiol. 2023 Jun;32(3):119-132.
pISSN 1226-2560 • eISSN 2093-8144

Original Article

Experimental Neurobiology

A Glimpse into the Genome-wide DNA Methylation Changes in 6-hydroxydopamine-induced *In Vitro* Model of Parkinson's Disease

Kasthuri Bai Magalingam[1], Sushela Devi Somanath[2] and Ammu Kutty Radhakrishnan[1]*

[1]Jeffrey Cheah School of Medicine and Health Sciences, Monash University, Bandar Sunway 47500, [2]Pathology Division, School of Medicine, International Medical University, Kuala Lumpur 57000, Malaysia

A cell-based model of Parkinson's disease (PD) is a well-established *in vitro* experimental prototype to investigate the disease mechanism and therapeutic approach for a potential anti-PD drug. The SH-SY5Y human neuroblastoma cells and 6-OHDA combo is one of the many neurotoxin-induced neuronal cell models employed in numerous neuroscience-related research for discovering neuroprotective drug compounds. Emerging studies have reported a significant correlation between PD and epigenetic alterations, particularly DNA methylation. However, the DNA methylation changes of PD-related CpG sites on the 6-OHDA-induced toxicity on human neuronal cells have not yet been reported. We performed a genome-wide association study (GWAS) using Infinium Epic beadchip array surveying 850000 CpG sites in differentiated human neuroblastoma cells exposed to 6-OHDA. We identified 236 differentially methylated probes (DMPs) or 163 differentially methylated regions (DMRs) in 6-OHDA treated differentiated neuroblastoma cells than the untreated reference group with $p<0.01$, Δbeta cut-off of 0.1. Among 236 DMPs, hypermethylated DMPs are 110 (47%), whereas 126 (53%) are hypomethylated. Our bioinformatic analysis revealed 3 DMRs that are significantly hypermethylated and associated with neurological disorders, namely AKT1, ITPR1 and GNG7. This preliminary study demonstrates the methylation status of PD-related CpGs in the 6-OHDA-induced toxicity in the differentiated neuroblastoma cells model.

Key words: Parkinson's disease, DNA methylation, GWAS, Neuroblastoma

INTRODUCTION

The SH-SY5Y human neuroblastoma cell line serves as a model for neurodegenerative diseases since the cells can be differentiated to mature neurons by culturing with specific compounds. Although the neuroblastoma cells possess some basic qualities of human neurons, the active proliferation feature of the cells does not seem to be a characteristic of neurons. Since neurons are cells that are regarded as postmitotic and do not proliferate once they are terminally differentiated. Therefore, most recent studies are emphasizing the need to differentiate the neuroblastoma cells to develop homogenous neurons that exhibit morphology and biochemical characteristics of neurons. Consistent with this, we have reported that differentiated neuroblastoma cells exhibited dopaminergic neuron characteristics with increased in neurite projections, dopamine neurotransmitters, α-synuclein neuroprotein and up-regulation of dopamine receptor D2 expression when maintained in low serum retinoic acid culture medium. Our study also showed that differentiated neuroblastoma cells were more susceptible to 6-hydroxydopamine (6-OHDA) than undifferentiated neuroblastoma cells [1]. The neurotoxin 6-OHDA has significantly contributed to developing a new drug therapy for PD. It has the structural analogue of catecholamines, dopamine and noradrenaline and able to exert a potent toxic effect on cat-

Submitted August 25, 2022, Revised April 6, 2023,
Accepted May 5, 2023

*To whom correspondence should be addressed.
TEL: 60-355144902, FAX: 60-355144902
e-mail: ammu.radhakrishnan@monash.edu

echolaminergic neurons [2]. The 6-OHDA has been frequently used *in vitro* experiments to induce apoptosis on neuroblastoma cells and mimic PD in a cellular model. The 6-OHDA and human neuroblastoma combo has been widely established and accepted in neuroscience research as an *in vitro* platform to understand a new drug's toxicity and protective mechanism before embarking on clinical research. Neuroprotective effects of numerous plant extracts [3], flavonoids [4], vitamins [5] and phytonutrients [6] have been elucidated using the 6-OHDA and SH-SY5Y neuroblastoma cells.

Various mechanisms have been suggested in the 6-OHDA-induced toxicity of neuroblastoma cells. A recent study reported that 6-OHDA-induced toxicity resulted in degradation of Cu (copper) exporter ATP7A and Cu chaperone Atox1, leading to disruption of cellular Cu trafficking. Moreover, 6-OHDA has been found to attenuate the Cu proenzyme dopamine β-hydroxylase that converts dopamine to noradrenaline [7]. Using quantitative proteomic analysis, our research group has documented that the 6-OHDA induced apoptosis remarkably upregulated the expression of VDAC1 and 17 histone proteins via overexpression of nucleosomal degradation pathways in differentiated neuroblastoma cells [8]. Besides that, He et al., have shown that 6-OHDA impairs the autophagic flux by downregulating the transcription factor EB (TFEB), a critical component controlling lysosome biogenesis. These damaging effects of 6-OHDA significantly reduce the expression of lysosome-associated membrane protein 1 (Lamp1) and the lysosomal proteases activity [9].

However, evidence of the epigenetic changes induced by 6-OHDA in *in vitro* PD model remains void. Epigenetic changes can be defined as any alterations in the gene expression pattern following DNA methylation, acetylation, phosphorylation, ubiquitylations or sumolyation that do not change the sequence of DNA building blocks. The well-studied epigenetic modification is DNA methylation [10]. In the DNA methylation process, DNA methyltransferase covalently transfers a methyl group to the C-5 position of the cytosine ring in CpG dinucleotide region of DNA. The genome region with the largest number of CpG dinucleotide repeats is known as CpG islands (CGI), spanning 1000~1500 base pairs (bp) in length. CGI shores and shelves are defined as 2-kb and 4-kb long bp covering both sides of CGI. Studies have shown that the epigenetic signature in disease may spread in any CpG region, including islands, shore, shelf or open seas (outside CGI regions). Furthermore, DNA methylation may occur in various gene areas, including upstream/downstream regions of the transcription start site (TSS), 3'UTR (untranslated region), 5'UTR, exon, gene body and introns [11]. A recent study has demonstrated that hypomethylation (most cytosines do not have 5-mC compared to control) of the promoter, first exon, 5'UTR, sixth exon, N_shore and S_Shore resulted in promotion of key oncogenes, that lead to onset of cancer [12]. In regards to PD, a genome-wide study has revealed DNA methylation changes in brain tissues obtained from PD patients compared to healthy individuals. In this study, a total of 234 significant DMRs were identified in the dorsal motor nucleus of the vagus nerve, with 44 in the substantia nigra and 141 in the cingulate gyrus were discovered in PD patients [13]. Therefore, it is essential to understand if DNA methylations in the human brain also exist in the cellular model widely used in the investigation of PD. A new drug that could reverse the DNA methylation manifested in the PD model and protect neuronal cells may have a promising outcome as a potential drug for the treatment or management of PD.

In the present study, we first developed the differentiated neuroblastoma cells and subsequently exposed the cells to 6-OHDA to create a PD model. Then, the cells were subjected to Illumina Human DNA methylation EPIC BeadChip assay and data were preprocessed in Genome. Studio and analysed using R Bioconductor minfi package. We generated the CpG probes that displayed significant differences from the control group and analyzed these CpG probes using the Metascape bioinformatic tool. Our finding revealed the overrepresentation of significant PD-related CpGs that play crucial roles in neuron growth, metabolism, calcium signaling and survival mechanism.

MATERIALS AND METHODS

Cell culture

The SH-SY5Y human neuroblastoma cells (Cat # CRL-2266) were cultured in a complete culture medium containing 88% of Dulbecco Modified Eagle Medium (DMEM) supplemented with 4.5 g/L glucose and L-glutamine without sodium pyruvate (Corning, Corning, NY, U.S.A), 10% heat-inactivated fetal bovine serum (FBS, Biosera, Nuaille, France), 1% Penicillin-streptomycin (P/S) (Gibco, Carlsbad, U.S.A) and 1% non-essential amino acid (NEAA, GIBCO, Carlsbad, U.S.A) 37°C in a humidified 5% CO_2 incubator. The culture medium was replaced every alternate day, and cells were sub-cultured at 70% confluence.

Differentiation of human neuroblastoma cells

The differentiated neuroblastoma cells were established by seeding 1×10^5 cells/ml of neuroblastoma cells in a complete culture medium in a T75 flask. After 24 hours of cell seeding, the cells were exposed to a differentiation medium containing 95% DMEM, 3% heat-activated FBS, 1% P/S, 1% NEAA and 10 μM of all-trans-retinoic acid (RA, Sigma Aldrich, St. Louis, U.S.A) for 6-days. After 6-days of incubation in differentiating medium, the differentiated

https://doi.org/10.5607/en22035

neuroblastoma cells expresses dopaminergic characteristics at morphological, biochemical and genetic levels [1].

Preparation and treatment protocol of 6-OHDA

On day 7 (after the 6-days of differentiation phase), the differentiated neuroblastoma cells were exposed to a culture medium containing 40 μM of 6-OHDA (Sigma Aldrich, St. Louis, U.S.A) for 24 hours. The concentration of 40 μM of 6-OHDA was selected based on the preliminary studies that demonstrated significant inhibition (IC50) on differentiated human neuroblastoma cells. The DNA extraction was performed after 24 hr treatment of differentiated neuroblastoma cells with 6-OHDA.

Extraction and purification of genomic DNA

DNA extraction was performed on untreated differentiated neuroblastoma cells (Neg Control) and differentiated neuroblastoma cells treated with 6-OHDA using the Lucigen MasterPure DNA purification kit (Thermofisher, MA, USA). Briefly, the untreated and 6-OHDA treated differentiated neuroblastoma cells were pelleted by centrifugation and the supernatant removed, leaving approximately 25 μl of liquid in each tube. The tubes were vortexed for 10 s to resuspend the cells and 300 μl of tissue and cell lysis solution containing 1 μl of Proteinase K (*provided with the kit*) was added to each tube. The tubes were mixed thoroughly and incubated at 65°C for 15 minutes, accompanied with a vortex mix every 5 minutes. Following this, the samples were cooled to 37°C and 1 μl of 5 μg/μl RNAase A (*provided with the kit*) was added to each tube. The tubes were mixed thoroughly and incubated at 37°C for 30 minutes. The tubes were placed on ice for 3~5 minutes before the DNA precipitation step.

To precipitate total DNA, 175 μl of MPC protein precipitation reagent (*provided with the kit*) was added to each tube containing the lysed samples. Then, the tubes were vortexed vigorously for 10 s and centrifuged (≥10,000 g) for 10 minutes at 4°C. The supernatant from each tube was transferred to a microcentrifuge tube and 500 μl of isopropanol (Sigma-Aldrich, St. Louis, USA) was added to the recovered supernatant. The tubes were inverted several times and centrifuged (≥10,000 g) for 10 minutes at 4°C to pellet total DNA in each sample. After centrifugation, the isopropanol was carefully discarded without dislodging the DNA pellet. The DNA pellet was rinsed with 70% ethanol and the residual ethanol was removed entirely from the tube. Finally, the DNA was resuspended in 35 μl of TE buffer (*provided with the kit*). The purity and quality of the extracted DNA were determined using a Nanoquant spectrophotometer (A260/A280 >1.8 & <2.1) and validated with agarose gel electrophoresis (no dispersion DNA fragment band). The extracted genomic DNA (gDNA) was stored at -80°C prior to use.

Genomic DNA bisulphite conversion

The purified gDNA samples were thawed to room temperature before the bisulphite conversion procedure using the EZ DNA Methylation Kit (Zymo Research, CA, USA). To initiate the bisulphite conversion step, 5 μl of M-dilution buffer (*provided with the kit*) was added to the 1 μg DNA sample (20 ng/μl). The samples were mixed by pipetting and incubated at 37°C for 15 minutes. Following this, 100 μl of the prepared CT conversion reagent (*provided with the kit*) was added to each tube and mixed thoroughly. The tubes were incubated in a thermocycler at 95°C for 30 sec, 50°C for 60 min for 16 cycles, then "hold" at 4°C. Next, 400 μl of M-binding buffer (*provided with the kit*) was added to Zymo-Spin IC columns (*provided with the kit*) and each column was placed into a collection tube. The columns were appropriately labelled. The samples were loaded into the respective Zymo-Spin IC column containing the M-Binding buffer and mixed by inverting the column. Then, the columns in the collection tubes were centrifuged (≥10,000 g for 30 seconds). The flow-through was discarded and 100 μl of M-Wash buffer (*provided with the kit*) was added to the columns and the columns were centrifuged (≥10,000 g for 30 seconds). Following this, 200 μl of M-Desulphonation buffer (*provided with the kit*) was added to each column. The columns were left at room temperature for 15~20 minutes and centrifuged (≥10,000 g for 30 seconds). The flow-through was discarded and 200 μl of M-Wash buffer was added to the column and centrifuged (≥10,000 g for 30 seconds). The wash step was repeated again. Finally, the column was placed into an appropriately labelled sterile 1.5 ml tube and 10 μl of M-Elution buffer (*provided with the kit*) was added to the column matrix. The column was centrifuged (≥10,000 g for 30 seconds) and the eluted DNA was stored at -20°C until further use.

Infinium human methylation Epic BeadChip methylation measurements

The methylation level of 865 918 CpGs in the human genome was assessed on 1 μg of bisulphite-converted gDNA using the Human DNA methylation EPIC BeadChip according to the Infinium Methylation Assay Protocol. The 6 samples were equally loaded in the EPIC Beadchip to prevent the batch effect. Assayed bead chips were scanned to generate the data in the form of .idat files for each biological sample via Illumina's GenomeStudio software. Following this, the .idat files were further processed using the R (4.1.2)/Minfi Bioconductor package (The R Project for Statistical Computing, Auckland, New Zealand). The β-value between 0 (totally unmethylated) and 1 (totally methylated) were generated after the

background subtraction of control probes, followed by normalization with a subset quantile normalization (SWAN) [14]. The quality control procedure eliminated the ensuing probes: i) probes with sex-specific CpG loci, ii) probes with a detection rate at p>0.01, iii) probes containing SNP. After these steps, 715 810 probes from a total of 865 918 CpG probes remained for methylome-wide analysis [15]. The DMPs between untreated control and 6-OHDA treated group were determined using dmpFinder algorithm from the *minfi* package in R Bioconductor. A pooled t-test, with a p value of ≤0.01 level of significance; bootstrapping, 300 (iterations), smoothing; between untreated and 6-OHDA treated group was applied as a cut-off. CpGs with average Δbeta (delta beta; difference in beta values between 6-OHDA treatment and untreated control group) of >0.1 was regarded as hypermethylation and Δbeta value <-0.1 being hypomethylation [16]. A chromosomal distribution and volcano plot depicting the difference in the methylation between 6-OHDA and the control groups (p<0.01) were generated using R Bioconductor Minfi package.

Bioinformatic analysis

The statistically significant DMRs with p<0.01 and Δbeta values cut-off of 0.1 were imputed into the Metascape tool (http://metascape.org/gp/index.html) for elucidation of gene ontology (GO) using GO biological Processes, KEGG, REactome Gene Sets, Canonical Pathways, PANTHER Pathway, CORUM and WikiPathways. The p values between the GO ontology clusters were calculated using hypergeometric distribution, while q-values were calculated using the Benjamini-Hochberg procedure to account for multiple tests. Then, the protein-protein interaction (PPI) enrichment analysis for the significant genes was performed using STRING, BioGrid, OmnoPath and InWeb_IM databases. The Molecular Complex Detection (MCODE) algorithm has been applied for a network that contains between 3 and 500 proteins. The best scoring terms by p values for each MCODE were identified as the functional description of each component [17].

Statistical analysis

The statistical difference between the study variables (untreated vs. 6-OHDA) was analysed using the R Bioconductor package minfi [18]. The CpG probes that demonstrated Δbeta <-0.1 (hypomethylated) and >0.1 (hypermethylated) with p<0.01 between 6-OHDA-treated and untreated differentiated neuroblastoma cells groups were regarded as statistically significant.

RESULTS

Genome-wide association analyses of 6-OHDA induced cytotoxicity in differentiated neuroblastoma cells

To determine the differences in the DNA methylome between untreated and 6-OHDA treated differentiated neuroblastoma cells, we performed genome-wide DNA methylation using the Infinium MethylationEPIC beadchip method. Among 865 918 CpG probes interrogated, 715 810 CpG probes were obtained after data filtration and normalization using the R Bioconductor/Minfi package. Then, these CpGs were further processed using the minfi package, and we discovered that 236 DMPs or 163 DMRs were significantly methylated by 6-OHDA with Δbeta cut-off 0.1 and p<0.01. The Manhattan plot of -log10 transformed p values of the 715 810 CpG probes at respected chromosomes is shown in Fig. 1A. This plot shows the distribution of DNA methylation changes induced by 6-OHDA in differentiated neuroblastoma cells across all chromosomes, except the sex chromosomes. The grey line indicates the cut-off of statistical significance of $p<1\times10^{-3}$ and the red line indicates $p<1\times10^{-5}$.

The volcano plot in Fig. 1B shows the bird's view visualization of DNA methylation changes in 6-OHDA exposed differentiated neuroblastoma cells. The volcano plot shows the log2 fold change of DMPs against -log10 (p values). Among 236 significant DMPs, 62 CpG probes displayed log2 (fold change) of more than 0.2, and 75 CpG sites with log2 (fold change) of less than -0.2.

We also explored the genomic distribution of the differentially methylated CpGs in relation to UCSC (University of California, Santa Cruz) CpG island (Shelf, shore, island, open seas) in 6-OHDA treated differentiated human neuroblastoma cells compared to the reference group as shown in Fig. 2A. The differentially methylated CpGs were overrepresented in open seas (65%) and under-represented in N_Shelf (1%) and S_Shelf (2%). We also investigated the methylation patterns at the UCSC refgene groups. The ref gene groups explored were the gene body, ExonBand (Exon boundary), TSS200 (within 200 bases of transcription start sites), TSS1500 (within 1500 bases of transcription start site), 5'UTR (5'-untranslated region) and 3'UTR (3'-untranslated region). Our data displayed that the CpG methylation was overrepresented at the gene body (80 CpG sites) and underrepresented at the ExonBand (3) and 3'UTR (5) regions (Fig. 2B).

We identified the top 10 hyper- and hypomethylated CpG sites with p<0.01 in 6-OHDA-treated differentiated neuroblastoma cells, as shown in Table 1 and 2. In the top 10 hypermethylated CpGs, 3 CpGs are from chromosome 3, in which two CpGs are from the gene body and one from 5'UTR. The top 5 hypermethylated CpGs with p<0.01, Δbeta>0.1 are ABHD5 (0.3), ITPR1 (0.29),

https://doi.org/10.5607/en22035

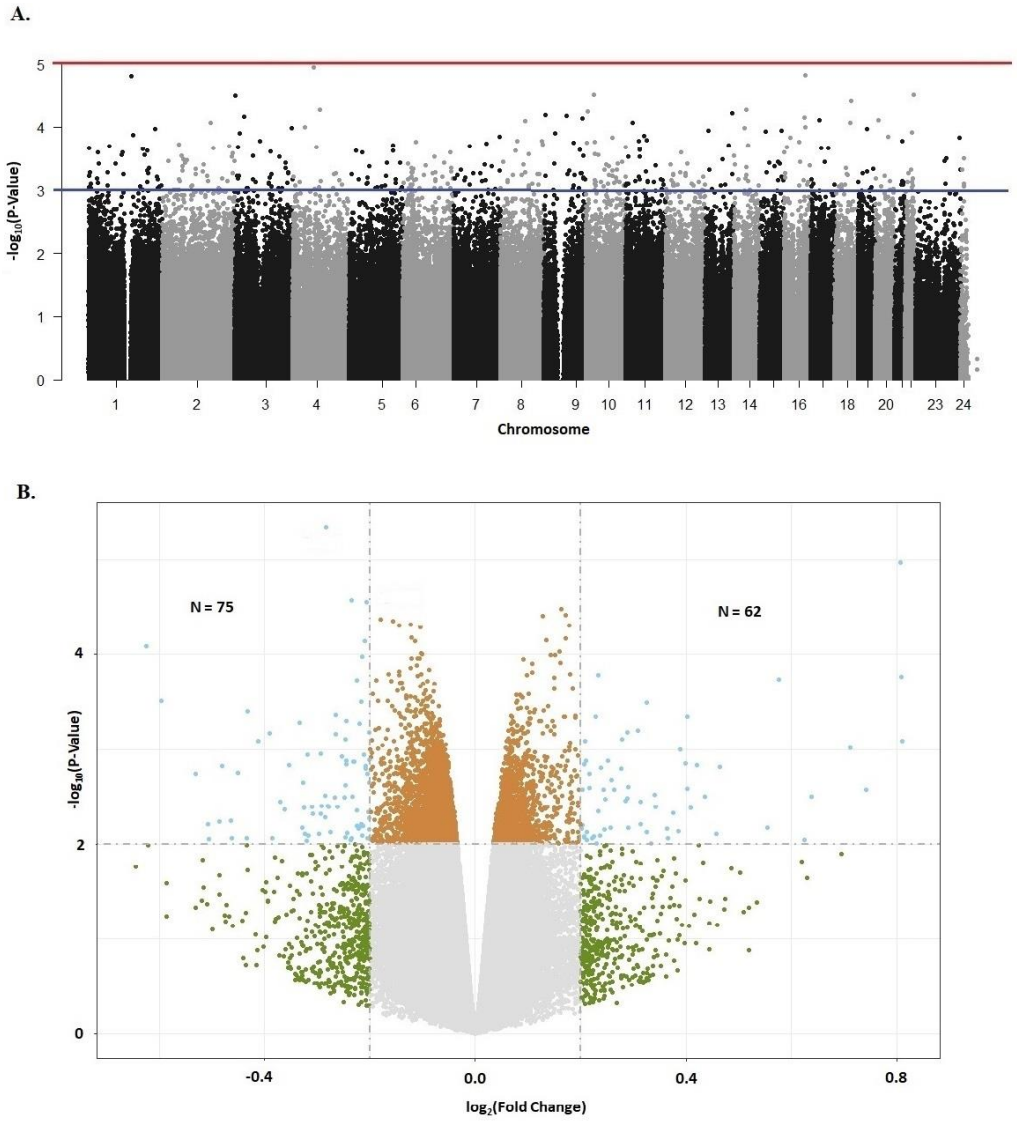

Fig. 1. Distribution of CpG probes in a cellular model of PD. (A) Manhattan plot of negative logarithm p values plotted against different chromosome positions. The grey line indicates a suggestive threshold, $p=1\times10^{-3}$, while the red line specifies a genome-wide significant threshold $p=1\times10^{-5}$. (B) Volcano plot of genome wide DNA methylation of 6-OHDA on differentiated human neuroblastoma cells. The x-axis shows log2 (fold change) values and the y axis plots the negative logarithm p values.

NRBP1 (0.26), ARID1B (0.26) and FADS3 (0.26) gene regions. Of note, ABHD5 (α/β-Hydrolase Domain Containing 5, Lysophosphatidic Acid Acyltransferase) gene is a key gene that encodes a protein that activates an enzyme called triglyceride lipase (ATGL). The ATGL is an important triacylglycerol (TG) hydrolase that catalyzes the generation of glycerol and free fatty acids. Mutation in this gene causes the pathologic accumulation of TG and leads to detrimental changes in neurons, such as a lack of axon regeneration and poor neuronal outcomes [19]. Hence, the hypermethylation of the ABHD5 gene body in the 6-OHDA-induced differentiated neuroblastoma cells may indicate lipid metabolism defects in neurons. In hypomethylated CpGs, nine out of ten CpGs are hypomethylated at the gene body. The top five hypomethylated CpG are RAD51B (-0.15), PMS1 (-0.15), C11orf49 (-0.13), STRN (-0.12) and SHISA7 (-0.11). Interestingly, the top hypomethylated CpG, RAD51B is a DNA repair gene that maintains genetic stability during the cell cycle [20]. Since DNA damage is one of the biochemical hallmarks in oxidative stress-induced apoptosis, the differential methylation of DNA repair genes may be an indication of differential gene regulation to counteract the cell death in the PD model.

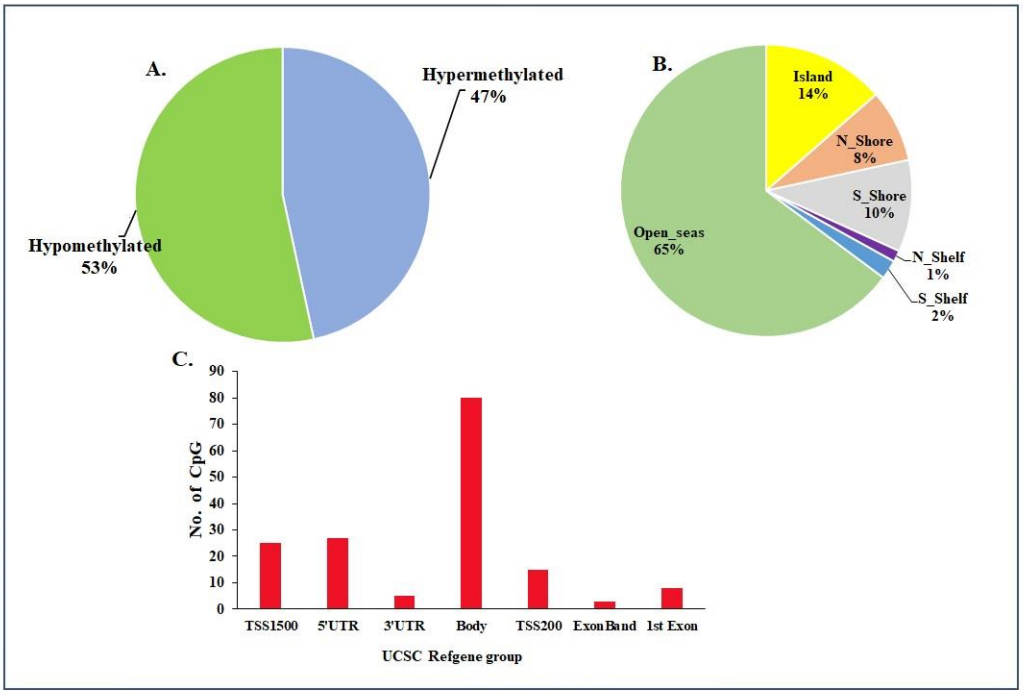

Fig. 2. GWAS results for CpG methylation analyses in 6-OHDA induced PD cell-based model compared to an untreated reference group with p<0.01. (A) Distribution of CpGs relative to CpG island. (B) Distribution of CpGs relative to gene regions.

Table 1. Top 10 significantly hypermethylated DMRs (Δbeta>0.1) in 6-OHDA treated differentiated neuroblastoma cells with p<0.01

TargetID	Δbeta	p value	FDR-q value	CHR	UCSC refgene name	UCSC refgene accession	UCSC refgene group	Relation to UCSC CpG island
cg23854042	0.30	0.004	0.902	3	ABHD5	NM_016006	Body	S_Shelf
cg12534855	0.29	0.002	0.848	3	ITPR1	NM_001099952	Body	
cg25828097	0.26	0.003	0.897	2	NRBP1	NM_013392	ExonBnd	
cg26307233	0.26	0.009	0.882	6	ARID1B	NM_020732	Body	
cg22837486	0.26	0.008	0.888	11	FADS3	NM_021727	1stExon	Island
cg01389693	0.26	0.001	0.852	4	UGT2A2	NM_001105677	TSS200	
cg15945942	0.26	0.001	0.851	1	DCAF8	NR_028103	Body	N_Shore
cg18309518	0.25	0.003	0.901	4	FRAS1	NM_001166133	Body	
cg02636380	0.24	0.001	0.854	11	C11orf88	NM_001100388	Body	
cg26074575	0.24	0.009	0.882	3	FNDC3B	NM_022763	5'UTR	

Table 2. Top 10 significantly hypomethylated DMRs (Δbeta>-0.1) in 6-OHDA treated differentiated neuroblastoma cells with p<0.01

TargetID	Δbeta	p value	FDR-q value	CHR	UCSC refgene name	UCSC refgene accession	UCSC refgene group	Relation to UCSC CpG island
cg12704715	-0.15311	0.008	0.885	14	RAD51B	NM_133510	Body	
cg11296782	-0.14491	0.005	0.899	2	PMS1	NM_001128143	Body	S_Shore
cg15921156	-0.13645	0.009	0.883	11	C11orf49	NR_103472	Body	
cg13402430	-0.12998	0.007	0.891	2	STRN	NM_003162	Body	
cg01603559	-0.11304	0.007	0.887	19	SHISA7	NM_001145176	Body	Island
cg09808639	-0.10808	0.002	0.847	10	GRK5	NM_005308	Body	
cg26837196	-0.10689	0.006	0.893	12	SPATS2	NM_023071	Body	
cg05906737	-0.10662	0.001	0.869	8	DOCK5	NM_024940	Body	
cg21127184	-0.10413	0.003	0.897	4	C4orf41	NM_021942	5'UTR	S_Shore
cg01024699	-0.10074	0.002	0.890	8	NECAB1	NM_022351	Body	

https://doi.org/10.5607/en22035

Bioinformatic analysis of differentially methylated regions regulated by 6-OHDA

The functional GO enrichment analysis (GO, KEGG, WikiPathways, Reactome terms) was conducted on the total set of 163 statistically significant DMRs as well as the hyper- and hypomethylated DMRs using Metascape bioinformatic database (Fig. 3). The overall DMRs analysis shows 20 GO-biological terms; whereby the top three overexpressed gene clusters included the regulation of neuron projection development (AKT1, ALK, BDNF, GAK, GRID2, IGF1R, SERPINI1, ROBO1, SDC2, BRSK2, CUX2, SI-

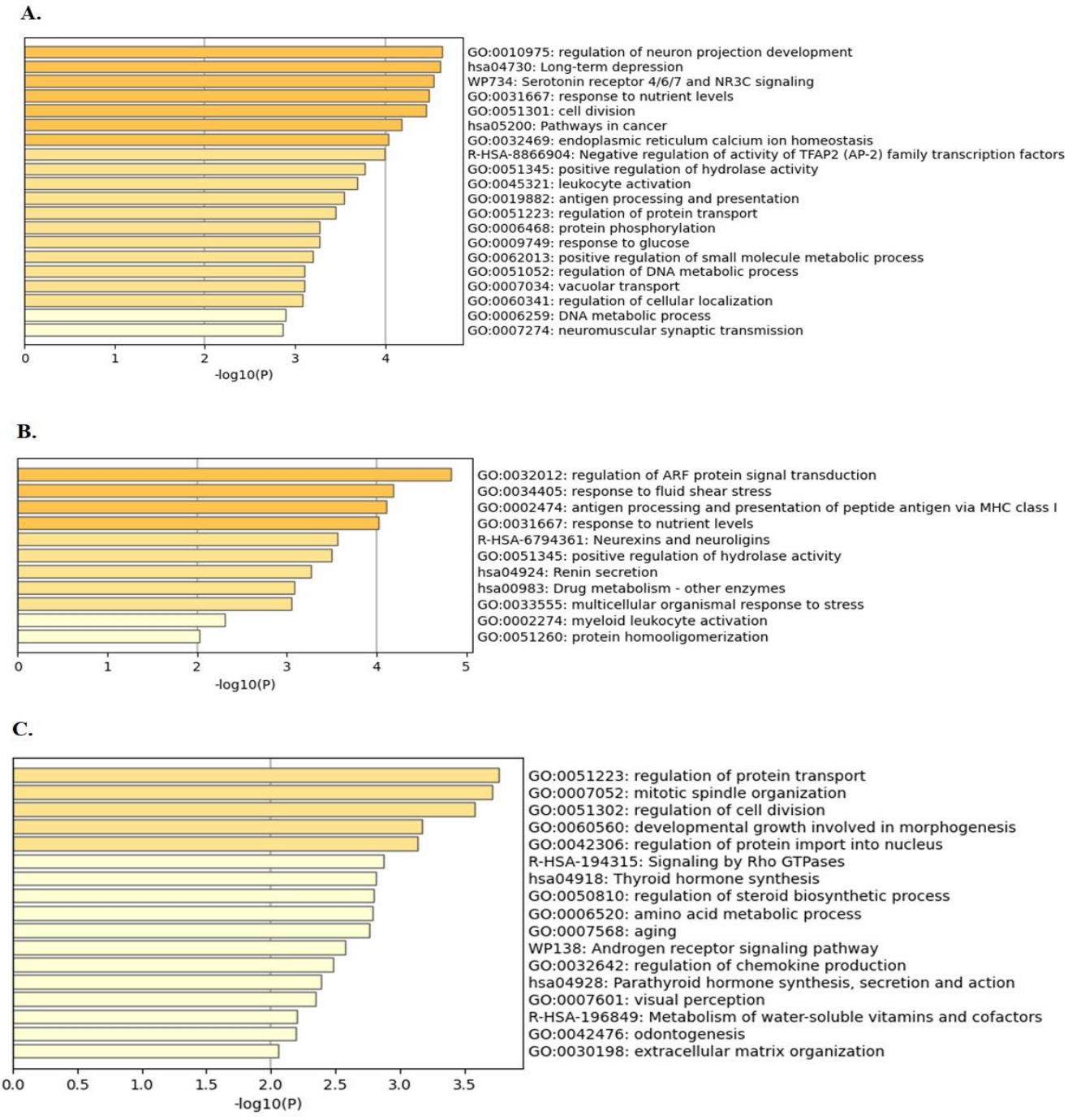

Fig. 3. Functional GO enrichment analysis of clustered enrichment ontology using Metascape on statistically significant DMRs in 6-OHDA induced differentiated neuroblastoma cells. (A) Functional GO analysis of 163 input DMRs. (B) Functional GO analysis of 71 hypermethylated DMRs. (C) Functional GO analysis of 92 hypomethylated DMRs.

PA1L1, SEMA5B, DDX56), long-term depression (GNAS, GRID2, IGF1R, ITPR1, PLCB4, MAPK1) and serotonin receptor 4/6/7 and NRC signaling (EGR1, GNAS, NR3C1, MAPK1). The enrichment of GO:0010975: regulation of neuron projection development reflects the significant methylation of genes modulating the rate or extend of neuron projection development regulated by 6-OHDA on differentiated neuroblastoma cells. Loss of dopaminergic innervation that disrupts striatal projection systems' response to cortical and thalamic signals has been evidenced in PD [21]. The discovery of differentially DNA methylated genes regulating the neuron projection development in our experimental model is crucial as it is congruent with the pathological event in PD (Fig. 3A).

The functional GO enrichment analysis on 71 hypermethylated genes depicted 11 GO-biological terms, with the top three overexpressed gene clusters including the regulation of ARF protein signal transduction (MAP4K4, IQSEC1, IQSEC3), response to fluid shear stress (AKT1, ACE, SOCS5) and antigen processing and presentation of peptide antigen via MHC class 1 (ACE, MICB, SAR1B) (Fig. 3B). Our study showed a significantly increased DNA methylation in genes regulating ARF (ADP-ribosylation factor) signal transduction that functions in recruiting cargo-sorting coat proteins to regulate membrane traffic and organelle structure and modulate membrane lipid composition via guanine nucleotide exchange. This data is in line with the identification of protein aggregates and fragmentation of the Golgi apparatus in the brain of PD and AD that is associated with the disruption in ARF GTPases membrane trafficking functions leading to neurodegeneration [22]. Therefore, we can conclude that the 6-OHDA-induced apoptosis in our study is mediated by changes in crucial regulator ARF GTPase proteins expression that disrupts constant membrane trafficking pathways in neurons and eliminates dysfunctional proteins [23].

We also conducted a functional GO enrichment analysis on 92 hypomethylated genes induced by 6-OHDA on differentiated neuroblastoma cells. Our analysis revealed 17 GO-biological terms, where the top three enriched gene clusters are regulation of protein transport (PIK3C3, SREBF1, SUMO1, GPR68, NROB3, HYAL2, SERGEF, RBM22), mitotic spindle organization (EML1, KIF2A, NEK6, CLASP1) and regulation of cell division (CXCR5, FGF1, PIK3C3, TP63, KIF13A) (Fig. 3B). The DNA methylation alteration of genes regulating protein transport within cells or between cells may cause disruption in protein translation, chaperone-assisted protein folding and protein degradation pathways [24].

We performed the PPI analysis on the 6-OHDA induced DNA methylation changes on 163 DMRs and obtained a rather messy hairball network (Fig. 4A). To further interpret the PPI, we focused on the MCODE algorithm with significant p values that was extracted by the database according to functional enrichment analysis. The input of 163 DMRs in the Metascape interface generated four MCODE modules that comprising 12 genes, from which 2 seed nodes were identified; ITPR1 and TDRD3. The seed proteins are proteins that are responsible in forming the clusters. The top three pathway clusters overexpressed in the MCODE 1 are three KEGG pathways that include Cholinergic synapse (hsa04725), dopaminergic synapse (hsa04728) and Apelin signaling pathway (hsa04371). The Cholinergic synapse pathway functions in formation, distribution and uptake of acetylcholine (ACh) neurotransmitter in neuronal synapse. In the human brain, ACh facilitates memory, learning and motor control [25]. Dopamine is generated in dopaminergic synapses and interacts with dopamine receptors in the central nervous system (CNS) to control locomotor, motivation, reward, sleep and endocrine regulation [26]. The Apelin signalling pathway is a neuronal survival response mechanism mediated by an endogenous native peptide ligand, Apelin [27]. The three genes that were differentially methylated in these three pathways are Inositol 1,4,5-triphosphate receptor type 1 (ITPR1), Guanine Nucleotide Binding Protein Subunit Gamma 7 (GNG7) and AKT Serine/Threonine Kinase 1 (AKT1) (Fig. 4B). The 3 GO terms/pathways displayed p values of less than 0.05, with cholinergic synapse expressing log10 p value=-7.3, dopaminergic synapse showing log10 p value=-7.1) and Apelin signaling pathway with log10 p value=-7.1 as curated by Metascape customized analysis (Fig. 4C). The increased DNA methylation levels on these genes in differentiated neuroblastoma cells exposed to 6-OHDA indicate the changes in gene regulation in these 3 pathways. Multitude studies have shown that progressive loss of synapses within striatum leads to neuronal loss in neurodegenerative diseases, such as PD [28]. Therefore, our findings have further confirmed that the loss of synapses in a neurodegeneration event may have association with changes in DNA methylations in genes involved in maintaining the number of axons and synapses for optimal function of neurons in central nervous system (CNS).

The other two pathways overexpressed by 6-OHDA are chromatin remodeling (GO:0006338) and chromatin organization (GO:0006325) in MCODE 2 module and protein phosphorylation (GO:0006468) processes in MCODE 3 modules.

The comparison of beta values of the ITPR1, AKT1 and GNG7 genes between 6-OHDA and neg control are illustrated in Fig. 5. All DMRs displayed an increased DNA methylation in 6-OHDA treated differentiated neuroblastoma cells compared to the negative control group. The Δbeta ITPR1 is 0.29 (p=0.002), Δbeta AKT1 is 0.11 (p=0.0000064) and Δbeta GNG7 is 0.1 (p=0.000198).

We further verified the overexpressed pathways by the 163

https://doi.org/10.5607/en22035

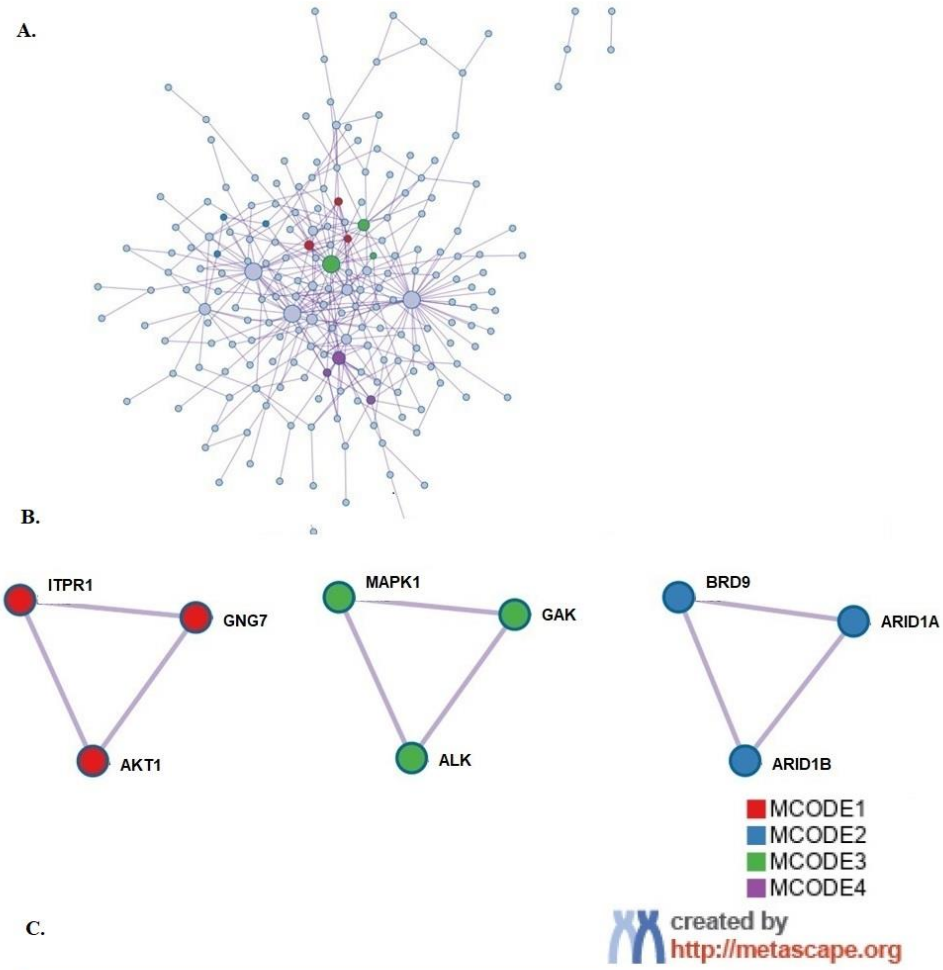

C.

Color	MCODE	GO	Description	Log10(P)
	MCODE_1	hsa04725	Cholinergic synapse	-7.3
	MCODE_1	hsa04728	Dopaminergic synapse	-7.1
	MCODE_1	hsa04371	Apelin signaling pathway	-7.0
	MCODE_2	GO:0006338	Chromatin remodeling	-6.0
	MCODE_2	GO:0006325	Chromatin organization	-5.1
	MCODE_3	GO:0006468	Protein phosphorylation	-4.9

Fig. 4. PPI network and overexpressed MCODE module regulated by 6-OHDA. (A) PPI visualized using MCODE algorithm where neighborhood densely connected DMRs were identified from clustered enrichment ontology terms. (B) MCODE1 consists of 3 genes, including ITPR1, GNG7, AKT1; MCODE2 consists of 3 genes, BRD9, ARID1A and ARID1B; MCODE3 consists of 3 genes, including MAPK1, GAK and ALK. (C) Description and p values of each MCODE network according to GO enrichment analysis.

significantly methylated DMRs in our 6-OHDA induced cytotoxicity on differentiated neuroblastoma cells using KEGG online database. Upon uploading the DMRs in the KEGG mapper interface, we found that the metabolic pathway was remarkably enriched with significant methylation of 12 DMRs, followed by neurodegeneration-multiple diseases (5 DMRs) and Ras signaling pathway (5 DMRs). Interestingly, we found that most of the DMRs were found in more than one pathway, such as GNG7 which was identified in the Ras signaling pathway, apelin signaling pathway and serotonergic synapse; AKT1 was enriched in Ras signaling pathway, Apelin signaling pathway, autophagy and cAMP signaling pathway; ITPR1 gene in pathways of neurodegeneration, apelin signaling pathway, autophagy, serotonergic synapse and calcium signaling pathway (Table 3). This data signifies the multiple roles these genes play in the biological pathways activated in the 6-OHDA-induced damage in differentiated neuroblastoma cells.

DISCUSSION

Epigenetic modification, particularly DNA methylation, is an indispensable molecular mechanism that occurs in response to genetics, environment, aging, diet and environmental toxins. Recently, studies have been directed to understanding the DNA methylation on PD-associated genes that alters the gene expression leading to neurodegeneration. An emerging study has confirmed that hypomethylation of cytochrome P450 2E1 (*CYP2E1*) gene was associated with increased expression of CYP2E1 protein in PD brains but not in blood cells and skin fibroblasts [29]. Considering the significance of DNA methylation in PD, we embarked on a study to investigate the DNA methylation alterations that arise in a cellular model of PD. However, the short-term treatment (24 h) of 6-OHDA on differentiated human neuroblastoma cells was expected to yield a mild to moderate level of methylation changes. Therefore, we report all CpG probes with Δbeta cut-off of 0.1 with p<0.01. Our finding showed that the 6-OHDA induced neurotoxicity model yielded significant DNA methylation changes on 236 CpG probes or 163 DMRs, p<0.01. Among these CpG probes, 110 CpGs were increased, while 126 decreased in DNA methylation level in 6-OHDA treated cells. The DNA methylation was primarily discovered in open sea region and gene body according to UCSC classification of CGI regions (Fig. 2B) and refgene groups (Fig. 2C), respectively.

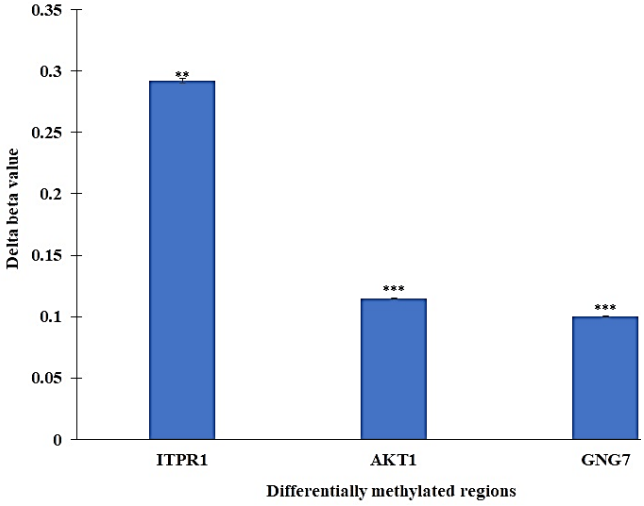

Fig. 5. Delta beta values of ITPR1, AKT1 and GNG7 as identified in MCODE 1 module. Data are expressed as mean±SEM, n=3. **p<0.01 and ***p<0.001 [6-OHDA vs. untreated control].

The 6-OHDA implicated DNA methylation changes on these 236 CpG probes was further scrutinized using Metascape, a web-based portal designed to provide functional gene annotation and unique pathways [30]. Our analysis revealed three significant DMRs (ITPR1, AKT1, GNG7) that are involved in three neuronal pathways as curated in KEGG pathway database, namely Cholinergic synapse (hsa04725), Dopaminergic synapse (hsa04728) and Apelin signaling pathway (hsa04371). These three genes are significantly hypermethylated by 6-OHDA than in negative control. The changes in DNA methylation levels in genes regulating the growth and maintenance of neuron synapses may alter the expression of these gene and eventually affects neuronal functions. Moreover, our study demonstrated that the neurodegeneration process in 6-OHDA-induced PD model is mediate by DNA methylation of critical genes that plays vital roles in cholinergic and dopaminergic synapse formation and functions.

ITPR1 is predominantly detected in the CNS and plays an im-

Table 3. Top overexpressed biological pathways obtained from KEGG Mapper

KEGG pathway	Genes
Metabolic pathway	*ALDH1L1*, *PDE10A*, *DPYD*, *PISD*, *GPX6*, *GBE1*, *PIK3C3*, *UGT2A2*, *NMNAT1*, *TK2*, *HYAL2*, *B3GALNT1*
Pathways of neurodegeneration - multiple diseases	*GPX6*, *APP*, *ITPR1*, *PIK2C3*, *ZFYVE1*
Ras signaling pathway	*AKT1*, *FGF1*, *GNG7*, *PAK6*, *ZAP70*
Apelin signaling pathway	*EGR1*, *AKT1*, *GNG7*, *ITPR1*, *PIK3C3*
Autophagy	*AKT1*, *ITPR1*, *PIK3C3*, *ZFYVE1*
cAMP signaling pathway	*PDE10A*, *ADRB1*, *AKT1*, *GNAS*
Serotonergic synapse	*GNAS*, *GNG7*, *APP*, *ITPR1*
Calcium signaling pathway	*ADRB1*, *FGF1*, *GNAS*, *ITPR1*

ALDH1L1, *aldehyde dehydrogenase 1 family member L1*; *PDE10A*, *phosphodiesterase 10A*; *DPYD*, *dihydropyrimidine dehydrogenase*; *PISD*, *phosphatidylserine decarboxylase*; *GPX6*, *glutathione peroxidase 6*; *GBE1*, *1,4-alpha-glucan branching enzyme 1*; *PIK3C3*, *phosphatidylinositol 3-kinase catalytic subunit type 3*; *UGT2A2*, *UDP glucuronosyltransferase family 2 member A2*; *NMNAT1*, *nicotinamide nucleotide adenylyltransferase 1*; *TK2*, *thymidine kinase 2*; *HYAL2*, *hyaluronidase 2*; *B3GALNT1*, *beta-1,3-N-acetylgalactosaminyltransferase*; *AKT1*, *AKT serine/threonine kinase 1*; *FGF1*, *fibroblast growth factor 1*; *GNG7*, *G protein subunit gamma 7*; *PAK6*, *p21 (RAC1) activated kinase 6*; *ZAP70*, *zeta chain of T cell receptor associated protein kinase 70*; *GPX6*, *glutathione peroxidase 6*; *APP*, *amyloid beta precursor protein*; *ITPR1*, *inositol 1,4,5-trisphosphate receptor type 1*; *ZFYVE1*, *zinc finger FYVE-type containing 1*; *EGR1*, *early growth response 1*; *PDE10A*, *phosphodiesterase 10A*; *ADRB1*, *adrenoceptor beta 1*; *GNAS*, *GNAS complex locus*.

https://doi.org/10.5607/en22035

portant role in regulating critical neuronal functions in synaptic plasticity and dendritic outgrowth [31]. Inositol 1,4,5-triphosphate receptors consist of a family of Ca^{2+} channels that regulate intracellular Ca^{2+} levels for physiological events to occur. We revealed that the 6-OHDA induced toxicity on differentiated neuroblastoma cells implicated significant DNA methylation changes (Δbeta=0.29, p=0.0019) on ITPR1 gene body-open seas. A previous study reported that misregulated DNA methylation cycle on ITPR1, caused downregulation of ITPR1 expression that resulted in cerebellar ataxia in murine model [32]. Furthermore, a compelling study has revealed that ITPR1-knock-out (KO) mice presented with severe cerebellar ataxia, opisthotonos, repetitive rigid posture and tonic contractions of the neck and trunk [33]. The role of ITPR1 in experimental PD has been well clarified by Fedorenko et al. According to their study, the 6-OHDA-induced state of experimental hemiparkinsonism in rats damaged the dopaminergic neurons of the substantia nigra and resulted in higher expression of ITPR1 gene. The overexpression of ITPR1 gene was associated with abnormal release of Ca^{2+} from intracellular calcium storage during the neurodegenerative process [34]. Aberrant Ca^{2+} levels in neurons affected by dysregulated ITPR1 has been identified as one of the possible mechanisms linking polyglutamine expansion of Huntingtin (Htt) protein and degeneration of GABAergic medium spiny striatal neurons in Huntington's disease [35].

The AKT1, a serine-threonine protein kinase, has been known for its role in cellular growth (division, differentiation), survival and apoptosis in neuronal cells. We showed that the 6-OHDA caused a significant increase in DNA methylation (Δbeta=0.11, p=0.0000064) at TSS1500-S shore compared to the control group. The effect of DNA shore methylation was reported in cancer research, whereby increased shore methylation alters tumor suppressor genes in breast tumors more than in normal tissue [36]. The effect of DNA methylation in AKT1 on gene expression was reported in a methamphetamine-induced psychosis study in human subjects. In this study, the DNA methylation on promoter regions of AKT1 was associated with increased expression of this gene in psychosis patients [37]. Nevertheless, compelling data from previous studies have suggested that AKT1 is involved in various signaling pathways that protect against PD [38]. Moreover, the previous study has shown that AKT activation is reduced in the PD brain, and its expression is mainly regulated by the PD-causing gene, *PINK1*. The lack of PINK1 activity causes the suppression of phospholipid PI (3,4,5)P_3 levels that give rise to fragmentation of Golgi apparatus, the pathological changes observed in PD. PINK1 gene protects Golgi apparatus from fragmentation through activation of AKT via kinase-dependent activity regulations of the primary activator, phospholipid PI(3,4,5)P_3 [39]. Besides that, Grider et al. have reported that increased activity of AKT in primary sensory neurons promotes dendritic branching and elongation via activation of localized Rac1 and mTOR signaling cascades [40]. Disruption in AKT activation or activity results in apoptosis in cultured neurons. At the same time, transfection of an active form of AKT promotes survival signaling pathway, neuron size and innervation of the striatum in postnatal development of dopamine neurons in mice [41].

The GNG7 encodes for γ7 protein that binds with the G-protein to form a heterotrimer ($G\alpha_{olf}\beta_2\gamma_7$) complex. The motor activity at the striatum is regulated via hierarchical assembly of the $G\alpha_{olf}\beta_2\gamma_7$ with dopamine receptor D_1 (DRD1) or adenosine A_{2A} receptor (AA2AR) that induce the activation of adenyl cyclase [42]. In our study, we showed a significant increase in DNA methylation at the 5'UTR-open seas region of GNG7 (Δbeta=0.1, p=0.000198). Although, no previous study reported on modulation of the GNG7 in neurological disorder, our bioinformatic analysis using Metascape tool has revealed a significant PPI in MCODE 1 interaction (Fig. 4). Nevertheless, a previous investigation by Schwindinger et al. on mice suggested that knock-down of GNG7 and GNG3 genes presented with a progressive seizure that declined the mice's life span to only 75 days. These effects were absent in a single knock-out of GNG7 or GNG3 gene alone which showed normal mice survival. This report concluded that the disparity in gene knock-down effects was attributed to the different functions elicited by G-protein constituted γ3 and γ7 subunits [43]. A compelling report from recent studies suggested that the selective loss of GNG7 (γ_7) gene expression disrupts the heterotrimer assembly of $G\alpha_{olf}\beta_2\gamma_7$, which affect the coupling with DRD1 or AA2AR receptors that interferes with the cAMP signaling and eventually compromises the downstream motor behaviors. It is important to note that dysfunction in the cAMP signaling in the human striatum has been associated with neurological or neurodegenerative diseases such as PD, dystonia, schizophrenia and drug addiction [44].

Although we are considered the pioneers in reporting the GWAS on DNA methylation in 6-OHDA induced PD cell-based model, this study was not without its limitations. Since this study was aimed to understand the different patterns of DNA methylation in PD-associated DMRs in the cellular model of PD, hence our data were not validated using other method. Secondly, the treatment duration with 6-OHDA on differentiated human neuroblastoma cells was only 24 hours. This protocol was well established for PD related studies [1]. As epigenetic changes require a sufficient amount of time to occur, we found the CpG methylation levels in our study were in the range of mild to moderate. Therefore, we set the Δbeta threshold as 0.1, with $p<0.01$ significance level. This

finding can serve as preliminary data for studies investigating the epigenetic changes implicated by therapeutic targets using a cell-based model of PD.

In conclusion, our study provides the first evidence for DNA methylation changes in the 6-OHDA induced cellular model of PD. Furthermore, our findings suggest that there was almost equal level of hypermethylation and hypomethylation in the identified DMPs. We also demonstrated that this experimental model significantly hypermethylated PD-related CpGs: AKT1, ITPR1 and GNG7.

ACKNOWLEDGEMENTS

This research was supported by JCSMHS internal grant scheme.

REFERENCES

1. Magalingam KB, Radhakrishnan AK, Somanath SD, Md S, Haleagrahara N (2020) Influence of serum concentration in retinoic acid and phorbol ester induced differentiation of SH-SY5Y human neuroblastoma cell line. Mol Biol Rep 47:8775-8788.
2. Simola N, Morelli M, Carta AR (2007) The 6-hydroxydopamine model of Parkinson's disease. Neurotox Res 11:151-167.
3. Kich DM, Bitencourt S, Alves C, Silva J, Pinteus S, Pedrosa R, Laufer S, de Souza CFV, Goettert MI (2016) Neuromodulatory effects of Calyptranthes grandifolia extracts against 6-hydroxydopamine-induced neurotoxicity in SH-SY5Y cells. Biomed Pharmacother 84:382-386.
4. Lee HJ, Noh YH, Lee DY, Kim YS, Kim KY, Chung YH, Lee WB, Kim SS (2005) Baicalein attenuates 6-hydroxydopamine-induced neurotoxicity in SH-SY5Y cells. Eur J Cell Biol 84:897-905.
5. Tang H, Zheng Z, Wang H, Wang L, Zhao G, Wang P (2022) Vitamin K2 modulates mitochondrial dysfunction induced by 6-hydroxydopamine in SH-SY5Y cells via mitochondrial quality-control loop. Nutrients 14:1504.
6. Magalingam KB, Somanath SD, Md S, Haleagrahara N, Fu JY, Selvaduray KR, Radhakrishnan AK (2022) Tocotrienols protect differentiated SH-SY5Y human neuroblastoma cells against 6-hydroxydopamine-induced cytotoxicity by ameliorating dopamine biosynthesis and dopamine receptor D2 gene expression. Nutr Res 98:27-40.
7. Kondo M, Hara H, Kamijo F, Kamiya T, Adachi T (2021) 6-Hydroxydopamine disrupts cellular copper homeostasis in human neuroblastoma SH-SY5Y cells. Metallomics 13:mfab041.
8. Magalingam KB, Somanath SD, Ramdas P, Haleagrahara N, Radhakrishnan AK (2022) 6-Hydroxydopamine induces neurodegeneration in terminally differentiated SH-SY5Y neuroblastoma cells via enrichment of the nucleosomal degradation pathway: a global proteomics approach. J Mol Neurosci 72:1026-1046.
9. He X, Yuan W, Li Z, Hou Y, Liu F, Feng J (2018) 6-Hydroxydopamine induces autophagic flux dysfunction by impairing transcription factor EB activation and lysosomal function in dopaminergic neurons and SH-SY5Y cells. Toxicol Lett 283:58-68.
10. Weinhold B (2006) Epigenetics: the science of change. Environ Health Perspect 114:A160-A167.
11. Jones PA (2012) Functions of DNA methylation: islands, start sites, gene bodies and beyond. Nat Rev Genet 13:484-492.
12. Liu YX, Li QZ, Cao YN (2022) The effect of key DNA methylation in different regions on gene expression in hepatocellular carcinoma. Mol Omics 18:57-70.
13. Young JI, Sivasankaran SK, Wang L, Ali A, Mehta A, Davis DA, Dykxhoorn DM, Petito CK, Beecham GW, Martin ER, Mash DC, Pericak-Vance M, Scott WK, Montine TJ, Vance JM (2019) Genome-wide brain DNA methylation analysis suggests epigenetic reprogramming in Parkinson disease. Neurol Genet 5:e342.
14. Fortin JP, Triche TJ Jr, Hansen KD (2017) Preprocessing, normalization and integration of the Illumina HumanMethylationEPIC array with minfi. Bioinformatics 33:558-560.
15. Lahtinen A, Puttonen S, Vanttola P, Viitasalo K, Sulkava S, Pervjakova N, Joensuu A, Salo P, Toivola A, Härmä M, Milani L, Perola M, Paunio T (2019) A distinctive DNA methylation pattern in insufficient sleep. Sci Rep 9:1193.
16. Wang J, Song H, Zhang Y (2021) Comprehensive analysis of gene expression and DNA methylation for preeclampsia progression. J Chin Med Assoc 84:410-417.
17. Magalingam KB, Somanath SD, Haleagrahara N, Selvaduray KR, Radhakrishnan AK (2022) Unravelling the neuroprotective mechanisms of carotenes in differentiated human neural cells: biochemical and proteomic approaches. Food Chem (Oxf) 4:100088.
18. Aryee MJ, Jaffe AE, Corrada-Bravo H, Ladd-Acosta C, Feinberg AP, Hansen KD, Irizarry RA (2014) Minfi: a flexible and comprehensive Bioconductor package for the analysis of Infinium DNA methylation microarrays. Bioinformatics 30:1363-1369.
19. Cerk IK, Wechselberger L, Oberer M (2018) Adipose triglyceride lipase regulation: an overview. Curr Protein Pept Sci 19:221-233.

20. Glendining KA, Markie D, Gardner RJ, Franz EA, Robertson SP, Jasoni CL (2017) A novel role for the DNA repair gene Rad51 in Netrin-1 signalling. Sci Rep 7:39823.
21. Zhai S, Tanimura A, Graves SM, Shen W, Surmeier DJ (2018) Striatal synapses, circuits, and Parkinson's disease. Curr Opin Neurobiol 48:9-16.
22. Kiral FR, Kohrs FE, Jin EJ, Hiesinger PR (2018) Rab GTPases and membrane trafficking in neurodegeneration. Curr Biol 28:R471-R486.
23. Arrazola Sastre A, Luque Montoro M, Lacerda HM, Llavero F, Zugaza JL (2021) Small GTPases of the Rab and Arf families: key regulators of intracellular trafficking in neurodegeneration. Int J Mol Sci 22:4425.
24. Lehtonen Š, Sonninen TM, Wojciechowski S, Goldsteins G, Koistinaho J (2019) Dysfunction of cellular proteostasis in Parkinson's disease. Front Neurosci 13:457.
25. Maurer SV, Williams CL (2017) The cholinergic system modulates memory and hippocampal plasticity via its interactions with non-neuronal cells. Front Immunol 8:1489.
26. Juárez Olguín H, Calderón Guzmán D, Hernández García E, Barragán Mejía G (2016) The role of dopamine and its dysfunction as a consequence of oxidative stress. Oxid Med Cell Longev 2016:9730467.
27. O'Donnell LA, Agrawal A, Sabnekar P, Dichter MA, Lynch DR, Kolson DL (2007) Apelin, an endogenous neuronal peptide, protects hippocampal neurons against excitotoxic injury. J Neurochem 102:1905-1917.
28. Reeve AK, Grady JP, Cosgrave EM, Bennison E, Chen C, Hepplewhite PD, Morris CM (2018) Mitochondrial dysfunction within the synapses of substantia nigra neurons in Parkinson's disease. NPJ Parkinsons Dis 4:9.
29. Kaut O, Schmitt I, Stahl F, Fröhlich H, Hoffmann P, Gonzalez FJ, Wüllner U (2022) Epigenome-wide analysis of DNA methylation in Parkinson's disease cortex. Life (Basel) 12:502.
30. Zhou Y, Zhou B, Pache L, Chang M, Khodabakhshi AH, Tanaseichuk O, Benner C, Chanda SK (2019) Metascape provides a biologist-oriented resource for the analysis of systems-level datasets. Nat Commun 10:1523.
31. Hisatsune C, Kuroda Y, Akagi T, Torashima T, Hirai H, Hashikawa T, Inoue T, Mikoshiba K (2006) Inositol 1,4,5-trisphosphate receptor type 1 in granule cells, not in Purkinje cells, regulates the dendritic morphology of Purkinje cells through brain-derived neurotrophic factor production. J Neurosci 26:10916-10924.
32. Kim J, Kim K, Mo JS, Lee Y (2020) Atm deficiency in the DNA polymerase β null cerebellum results in cerebellar ataxia and Itpr1 reduction associated with alteration of cytosine methylation. Nucleic Acids Res 48:3678-3691.
33. Hisatsune C, Mikoshiba K (2017) IP3 receptor mutations and brain diseases in human and rodents. J Neurochem 141:790-807.
34. Fedorenko OA, Mamontov SM, Kotik OA, Talanov SA (2014) Changes in the gene expression of inositol 1,4,5-trisphosphate receptors in neurons of the motor cortex and cerebellum of rats with experimental hemiparkinsonism. Neurophysiology 46:173-176.
35. Bezprozvanny I, Hayden MR (2004) Deranged neuronal calcium signaling and Huntington disease. Biochem Biophys Res Commun 322:1310-1317.
36. Muse ME, Titus AJ, Salas LA, Wilkins OM, Mullen C, Gregory KJ, Schneider SS, Crisi GM, Jawale RM, Otis CN, Christensen BC, Arcaro KF (2020) Enrichment of CpG island shore region hypermethylation in epigenetic breast field cancerization. Epigenetics 15:1093-1106.
37. Nohesara S, Ghadirivasfi M, Barati M, Ghasemzadeh MR, Narimani S, Mousavi-Behbahani Z, Joghataei M, Soleimani M, Taban M, Mehrabi S, Thiagalingam S, Abdolmaleky HM (2016) Methamphetamine-induced psychosis is associated with DNA hypomethylation and increased expression of AKT1 and key dopaminergic genes. Am J Med Genet B Neuropsychiatr Genet 171:1180-1189.
38. Xiromerisiou G, Hadjigeorgiou GM, Papadimitriou A, Katsarogiannis E, Gourbali V, Singleton AB (2008) Association between AKT1 gene and Parkinson's disease: a protective haplotype. Neurosci Lett 436:232-234.
39. Furlong RM, Lindsay A, Anderson KE, Hawkins PT, Sullivan AM, O'Neill C (2019) The Parkinson's disease gene *PINK*1 activates Akt via PINK1 kinase-dependent regulation of the phospholipid PI(3,4,5)P_3. J Cell Sci 132:jcs233221.
40. Grider MH, Park D, Spencer DM, Shine HD (2009) Lipid raft-targeted Akt promotes axonal branching and growth cone expansion via mTOR and Rac1, respectively. J Neurosci Res 87:3033-3042.
41. Ries V, Cheng HC, Baohan A, Kareva T, Oo TF, Rzhetskaya M, Bland RJ, During MJ, Kholodilov N, Burke RE (2009) Regulation of the postnatal development of dopamine neurons of the substantia nigra in vivo by Akt/protein kinase B. J Neurochem 110:23-33.
42. Schwindinger WF, Mihalcik LJ, Giger KE, Betz KS, Stauffer AM, Linden J, Herve D, Robishaw JD (2010) Adenosine A2A receptor signaling and golf assembly show a specific requirement for the gamma7 subtype in the striatum. J Biol Chem 285:29787-29796.
43. Schwindinger WF, Mirshahi UL, Baylor KA, Sheridan KM,

Stauffer AM, Usefof S, Stecker MM, Mirshahi T, Robishaw JD (2012) Synergistic roles for G-protein γ3 and γ7 subtypes in seizure susceptibility as revealed in double knock-out mice. J Biol Chem 287:7121-7133.

44. Brunori G, Pelletier OB, Stauffer AM, Robishaw JD (2021) Selective manipulation of G-protein γ7 subunit in mice provides new insights into striatal control of motor behavior. J Neurosci 41:9065-9081.

https://doi.org/10.5607/en22035